regions. Amino-acid side chains exhibiting weak electron density were built with steric and geometric constraints. We generated the figures with GRASP, Molscript and Raster3D.

Structural comparisons

We carried out structural comparisons against 251 Fab and 11 αβTCR models. Superpositions were performed using LSQMAN[28]. The inter-domain, intra-chain angles (for instance Vγ–Cγ) were calculated as the supplement of the rotation angle necessary for superposition of the conserved α-carbon atoms of the B and F strands of each domain. Because the Vγ–Vδ interface involves the A′GFCC′C″ β-sheet whereas the Cγ–Cδ interface involves the ABED β-sheet (Fig. 1), V domain strands B and F were explicitly superimposed onto C domain strands F and B. The elbow angle between the V and C domains was calculated as the angle between the pseudo-dyads, described by direction cosines, which result from a superposition of V or C domains. Buried interfaces were calculated with CNS using a probe radius of 1.4 Å. Structures of αβTCRs and Fabs are referred to by their Protein Data Bank identification codes (http://www.rcsb.org).

Received 16 January; accepted 30 April 2001.

1. Hayday, A. C. γδ cells: a right time and a right place for a conserved third way of protection. *Annu. Rev. Immunol.* **18,** 975–1026 (2000).
2. Chien, Y. H., Jores, R. & Crowley, M. P. Recognition by γ/δ T cells. *Annu. Rev. Immunol.* **14,** 511–532 (1996).
3. Constant, P. *et al.* Stimulation of human γδ T cells by nonpeptidic mycobacterial ligands. *Science* **264,** 267–270 (1994).
4. Rock, E. P., Sibbald, P. R., Davis, M. M. & Chien, Y. H. CDR3 length in antigen-specific immune receptors. *J. Exp. Med.* **179,** 323–328 (1994).
5. Sciammas, R. *et al.* Unique antigen recognition by a herpesvirus-specific TCR-γδ cell. *J. Immunol.* **152,** 5392–5397 (1994).
6. Morita, C. T. *et al.* Direct presentation of nonpeptide prenyl pyrophosphate antigens to human γδ T cells. *Immunity* **3,** 495–507 (1995).
7. Lang, F. *et al.* Early activation of human Vγ9Vδ2 T cell broad cytotoxicity and TNF production by nonpeptidic mycobacterial ligands. *J. Immunol.* **154,** 5986–5994 (1995).
8. Davodeau, F. *et al.* Close correlation between Daudi and mycobacterial antigen recognition by human γδ T cells and expression of V9JPC1γ/V2DJCδ-encoded T cell receptors. *J. Immunol.* **151,** 1214–1223 (1993).
9. Fournié, J. J. & Bonneville, M. Stimulation of γδ T cells by phosphoantigens. *Res. Immunol.* **147,** 338–347 (1996).
10. Belmant, C. *et al.* 3-formyl-1-butyl pyrophosphate: a novel mycobacterial metabolite-activating human γδ T cells. *J. Biol. Chem.* **274,** 32079–32084 (1999).
11. Tanaka, Y., Morita, C. T., Nieves, E., Brenner, M. B. & Bloom, B. R. Natural and synthetic non-peptide antigens recognized by human γδ T cells. *Nature* **375,** 155–158 (1995).
12. Bukowski, J. F., Morita, C. T. & Brenner, M. B. Human γδ T cells recognize alkylamines derived from microbes, edible plants, and tea: implications for innate immunity. *Immunity* **11,** 57–65 (1999).
13. Kunzmann, V. *et al.* Stimulation of γδ T cells by aminobisphosphonates and induction of antiplasma cell activity in multiple myeloma. *Blood* **96,** 384–392 (2000).
14. Li, H. *et al.* Structure of the Vδ domain of a human γδ T-cell antigen receptor. *Nature* **391,** 502–506 (1998).
15. Loh, E. Y. *et al.* Gene transfer studies of T cell receptor-γδ recognition. Specificity for staphylococcal enterotoxin A is conveyed by Vγ9 alone. *J. Immunol.* **152,** 3324–3332 (1994).
16. Li, H. *et al.* Three-dimensional structure of the complex between a T cell receptor β chain and the superantigen staphylococcal enterotoxin B. *Immunity* **9,** 807–816 (1998).
17. Morita, C. T. *et al.* Superantigen recognition by γδ T Cells: SEA recognition site for human Vγ2 T cell receptors. *Immunity* **14,** 331–344 (2001).
18. Belmant, C. *et al.* A chemical basis for selective recognition of nonpeptide antigens by human γδ T cells. *FASEB J.* **14,** 1669–1670 (2000).
19. Davodeau, F. *et al.* Peripheral selection of antigen receptor junctional features in a major human γδ subset. *Eur. J. Immunol.* **23,** 804–808 (1993).
20. Panchamoorthy, G. *et al.* A predominance of the T cell receptor Vγ2/Vδ2 subset in human mycobacteria-responsive T cells suggests germline gene encoded recognition. *J. Immunol.* **147,** 3360–3369 (1991).
21. Bentley, G. A., Boulot, G., Karjalainen, K. & Mariuzza, R. A. Crystal structure of the β chain of a T cell antigen receptor. *Science* **267,** 1984–1987 (1995).
22. Wang, J. *et al.* Atomic structure of an αβ T cell receptor (TCR) heterodimer in complex with an anti-TCR Fab fragment derived from a mitogenic antibody. *EMBO J.* **17,** 10–26 (1998).
23. Davodeau, F. *et al.* Secretion of disulfide-linked human T-cell receptor γδ heterodimers. *J. Biol. Chem.* **268,** 15455–15460 (1993).
24. Otwinowski, Z. & Minor, W. Processing of X-ray diffraction data collected in oscillation mode. *Methods Enzymol.* **276,** 307–326 (1997).
25. Smith, G. D., Nagar, B., Rini, J. M., Hauptman, H. A. & Blessing, R. H. The use of SnB to determine an anomalous scattering substructure. *Acta Crystallogr. D* **54,** 799–804 (1998).
26. de la Fortelle, E. & Bricogne, G. Maximum-likelihood heavy-atom parameter refinement for multiple isomorphous replacement and multiwavelength anomalous diffraction methods. *Methods Enzymol.* **276,** 472–494 (1997).
27. Bailey, S. The CCP4 suite—programs for protein crystallography. *Acta Crystallogr D* **50,** 760–763 (1994).
28. Kleywegt, G. J. & Jones, T. A. in *From First Map to Final Model* (eds. Bailey, S., Hubbard, R. & Waller, D.) 59–66 (SERC Daresbury Laboratory, Warrington, 1994).
29. Jones, T. A., Zou, J. Y., Cowan, S. W. & Kjeldgaard, M. Improved methods for binding protein models in electron density maps and the location of errors in these models. *Acta Crystallogr. A* **47,** 110–119 (1991).
30. Brünger, A. T. *et al.* Crystallography & NMR system: A new software suite for macromolecular structure determination. *Acta Crystallogr. D* **54,** 905–921 (1998).

Supplementary information is available on *Nature's* World-Wide Web site (http://www.nature.com) or as paper copy from the London editorial office of *Nature*.

Acknowledgements

We thank C. Hammer for mass spectrometry; M. Garfield for amino-acid sequencing; S. Garman for advice and discussions; and Z. Dauter and K. R. Rajashankar for help at beamline X9B at the National Synchrotron Light Source at Brookhaven National Laboratory, which is supported by the US Department of Energy, Division of Materials Sciences and Division of Chemical Sciences. T.J.A. is supported by a postdoctoral fellowship from the Cancer Research Institute. This work is supported by the intramural program of the National Institute of Allergy and Infectious Diseases.

Correspondence and requests for materials should be addressed to T.J.A. (e-mail: tallison@niaid.nih.gov) or D.N.G. (e-mail: garboczi@nih.gov).
Coordinates have been deposited at the Protein Data Bank (identification code 1hxm) and will be released on publication.

corrections

Plant diversity enhances ecosystem responses to elevated CO_2 and nitrogen deposition

Peter B. Reich, Jean Knops, David Tilman, Joseph Craine, David Ellsworth, Mark Tjoelker, Tali Lee, David Wedin, Shahid Naeem, Dan Bahauddin, George Hendrey, Shibu Jose, Keith Wrage, Jenny Goth & Wendy Bengston

Nature **410,** 809–812 (2001).

This paper should have included the following acknowledgement:

We thank the US Department of Energy for financial support, with additional support from the US National Science Foundation Long-Term Ecological Research Program. □

Enabling the chemistry of life

C. Walsh

Nature **409,** 226–231 (2001).

In Fig. 4 of this *Insight* article, the P450 haem active site is wrongly shown as a uroporphyrinogen I rather than a protoporphyrin IX macrocycle. The correct version of the molecule is shown here. □

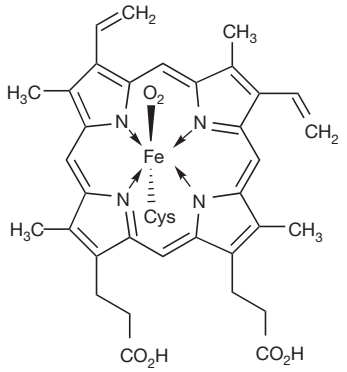

There is thus no need to invoke basal tractions due to subduction to explain pop-up structures, as has often been done for the western Americas[27,28,29].

The absence of slip beneath the Bhutan Himalaya in 1897 suggests that the 400-km region between the great Himalayan ruptures of 1934 and 1950 (Fig. 1) has remained a seismic gap for at least the past two centuries[30]. At the higher end of our estimated slip rates, the faults bounding the Shillong plateau could absorb one-third of the inferred Himalayan contraction rate of 18 mm yr^{-1} (ref. 31), correspondingly increasing the interval between great earthquakes in the Bhutan Himalaya.

Our conclusions also raise issues concerning the seismic hazard potential of the Shillong plateau. The >300-km length of the Dauki fault has not slipped recently, but were it to slip in a single earthquake its potential maximum magnitude ($M \geq 8$) would constitute a significant seismic threat to nearby densely populated regions of Bangladesh, and to the very large city of Dhaka less than 150 km to the south (Fig. 1). The interval between these giant plateau-building earthquakes fortunately exceeds 3,000 years. □

Received 1 September 2000; accepted 31 January 2001.

1. Oldham, R. D. Report on the Great Earthquake of 12 June 1897. *Mem. Geol. Soc. India* **29,** 1–379 (1899).
2. Seeber, L. & Armbruster, J. in *Earthquake Prediction: An International Review* (eds Simpson, D. W. & Richards, P. G. 259–277 (Maurice Ewing Series, Vol. 4, American Geophysical Union, Washington DC, 1981).
3. Molnar, P. & Pandey, M. R. Rupture zones of great earthquakes in the Himalayan Region. *Proc. Indian Acad. Sci. (Earth Planet. Sci.)* **98,** 61–70 (1989).
4. Molnar, P. The distribution of intensity associated with the great 1897 Assam earthquake and bounds on the extent of the rupture zone. *J. Geol. Soc. India* **30,** 13–27 (1987).
5. Gahalaut, V. K. & Chander, R. A rupture model for the great earthquake of 1897, northeast India. *Tectonophysics* **204,** 163–174 (1992).
6. Bond, J. in *Annual Report of Triangulation 1897–1898* (ed. Strahan, C.) Part II, xii–xiii (Survey of India Department, Calcutta, 1899).
7. Burrard, S. G. *Great Trigonometrical Survey of India, North East Longitudinal Series, Synoptical Volume 35* (Survey of India, Dehra Dun, 1909).
8. Wilson, C. A. K. *Triangulation of the Assam Valley Series, Geodetic Report 1938*, 10–22 (Survey of India, Dehra Dun, 1939).
9. Strahan, G. *Great Trigonometrical Survey of India, Assam Valley Triangulation, Synoptical Volume 32* (Survey of India, Calcutta, 1891).
10. Nagar, V. K., Singh, A. N. & Prakesh, A. Strain pattern in N. E. India inferred from geodetic triangulation data. *Mem. Geol. Soc. India* **23,** 265–273 (1992).
11. Frank, F. C. Deduction of earth strains from survey data. *Bull. Seismol. Soc. Am.* **56,** 35–42 (1966).
12. Okada, Y. Surface deformation due to shear and tensile faults in a half-space. *Bull. Seismol. Soc. Am.* **75,** 1135–1154 (1985).
13. Das, J. D., Saraf, A. K. & Jain, A. K. Fault tectonics of the Shillong Plateau and adjoining regions, northeast India, using remote sensing. *Int. J. Remote Sensing* **16,** 1633–1646 (1995).
14. Gomberg, J. & Ellis, M. Topography and tectonics of the central New Madrid seismic zone: results of numerical experiments using a three-dimensional boundary element program. *J. Geophys. Res.* **99,** 20299–20310 (1994).
15. Chen, W.-P. & Molnar, P. Source parameters of earthquakes and intraplate deformation beneath the Shillong Plateau and the northern Indoburman ranges. *J. Geophys. Res.* **95,** 12527–12552 (1990).
16. Le Dain, A. Y., Tapponier, P. & Molnar, P. Active faulting and tectonics of Burma and surrounding regions. *J. Geophys. Res.* **89,** 453–472 (1984).
17. Khattri, K. N. Seismological investigations in north eastern region of India. *Mem. Geol. Surv. India* **23,** 275–302 (1992).
18. Verma, R. K. & Mukhopadhay, M. An analysis of the gravity field in northeastern India. *Tectonophysics* **42,** 283–317 (1977).
19. Ambraseys, N. Reappraisal of North Indian earthquakes at the turn of the 20th century. *Current Sci.* **79,** 1237–1250 (2000).
20. Murthy, M. V. N., Talukdar, S. C., Bhattacharya, A. C. & Chakrabarti, C. The Dauki Fault of Assam. *Bull. Oil Natural Gas Commission* **6,** 57–64 (1969).
21. Johnson, S. J. & Alam, A. M. N. Sedimentation and tectonics of the Sylhet trough, Bangladesh. *Geol. Soc. Am. Bull.* **103,** 1513–1527 (1991).
22. Evans, P. The tectonic framework of Assam. *J. Geol. Soc. India* **5,** 80–96 (1964).
23. Paul, J. *et al.* Active deformation across India. *Geophys. Res. Lett.* **28,** 647–651 (2001).
24. Sukhija, B. S. *et al.* Timing and return of major paleoseismic events in the Shillong Plateau, India. *Tectonophysics* **308,** 53–65 (1999).
25. Rogers, J. Chains of basement uplifts within cratons marginal to orgenic belts. *Am. J. Sci.* **287,** 661–692 (1987).
26. Lyon-Caen, H. & Molnar, P. Gravity anomalies, flexure of the Indian Plate, and the structure, support and evolution of the Himalaya and Ganga basin. *Tectonics* **4,** 513–538 (1985).
27. Lipman, P. W., Protska, H. J. & Christiansen, R. L. Evolving subduction zones in the western United States, as interpreted from igneous rocks. *Science* **174,** 821–825 (1971).
28. Dickinson, W. R. & Snyder, W. S. Plate tectonics of the Laramide orogeny. *Geol. Soc. Am. Mem.* **151,** 355–366 (1978).
29. Jordan, T. E. *et al.* Andean tectonics related to the geometry of the subducted Nazca plate. *Geol. Soc. Am. Bull.* **94,** 341–361 (1983).
30. Bilham, R. & Gaur, V. K. The geodetic contribution to Indian seismotectonics. *Current Sci.* **79,** 1259–1269 (2000).
31. Bilham, R., Larson, K., Freymueller, J., & Project Idylhim members. GPS measurements of present-day convergence across the Nepal Himalaya. *Nature* **386,** 61–64 (1997).
32. Sibson, R. H. & Xie, G. Dip range for intracontinental reverse fault ruptures: the truth not stranger than friction. *Bull. Seismol. Soc. Am.* **88,** 1014–1022 (1998).

Acknowledgements

This work was funded by the National Science Foundation and the Natural Environment Research Council. R.B. received a John Simon Guggenheim Memorial Foundation fellowship while at Oxford University.

Correspondence and requests for materials should be addressed to R.B. (e-mail: bilham@stripe.colorado.edu).

Plant diversity enhances ecosystem responses to elevated CO_2 and nitrogen deposition

Peter B. Reich*, Jean Knops†, David Tilman†, Joseph Craine‡, David Ellsworth§, Mark Tjoelker*, Tali Lee*, David Wedin‖, Shahid Naeem†, Dan Bahauddin*, George Hendrey§, Shibu Jose*, Keith Wrage*, Jenny Goth* & Wendy Bengston*

* *Department of Forest Resources, University of Minnesota, St Paul, Minnesota 55108, USA*
† *Department of Ecology, Evolution and Behavior, University of Minnesota, St Paul, Minnesota 55108, USA*
‡ *Department of Integrative Biology, University of California, Berkeley, California 94720, USA*
§ *Division of Environmental Biology, Brookhaven National Laboratory, Upton, New York 11973, USA*
‖ *School of Natural Resource Sciences, University of Nebraska, Lincoln, Nebraska 68583, USA*

Human actions are causing declines in plant biodiversity, increases in atmospheric CO_2 concentrations and increases in nitrogen deposition; however, the interactive effects of these factors on ecosystem processes are unknown[1,2]. Reduced biodiversity has raised numerous concerns, including the possibility that ecosystem functioning may be affected negatively[1–4], which might be particularly important in the face of other global changes[5,6]. Here we present results of a grassland field experiment in Minnesota, USA, that tests the hypothesis that plant diversity and composition influence the enhancement of biomass and carbon acquisition in ecosystems subjected to elevated atmospheric CO_2 concentrations and nitrogen deposition. The study experimentally controlled plant diversity (1, 4, 9 or 16 species), soil nitrogen (unamended versus deposition of 4 g of nitrogen per m^2 per yr) and atmospheric CO_2 concentrations using free-air CO_2 enrichment (ambient, 368 μmol mol^{-1}, versus elevated, 560 μmol mol^{-1}). We found that the enhanced biomass accumulation in response to elevated levels of CO_2 or nitrogen, or their combination, is less in species-poor than in species-rich assemblages.

In the twenty-first century humans will live in, manage and depend on ecosystems that are less diverse[1,2] and subjected to higher CO_2 levels and nitrogen (N) deposition rates than in recorded human history[1]. Although we are beginning to understand the individual impacts of each of these factors on terrestrial ecosystems, our understanding of their interactive effects is poor at best[1–10]. Net primary productivity and carbon (C) input to ecosystems are usually enhanced by elevated CO_2, but this seems to be related to the extent and type of other limitations[11–20]. Nitrogen-poor ecosystems have often shown less response to elevated CO_2 than more fertile systems[18–25], which is important given that, worldwide,

productivity in most terrestrial ecosystems is limited by N (ref. 26) and rates of N deposition are expected to increase in the future[1,2,6]. In addition, it has been proposed that species-poor communities may be less responsive to elevated CO_2 or N compared with diverse communities[7].

Our study focuses on the influence of plant diversity on the response of ecosystem functions, such as productivity, to elevated CO_2 and N supply rates. Theoretically, because the range in plant traits associated with acquisition of C and N is frequently correlated with the species or functional diversity of an ecosystem[7,10], ecosystem responses to elevated CO_2 and N deposition may be sensitive to variation in levels of biodiversity[4,7,10,11,13–19]. High-diversity plant communities frequently have a greater range of plant functional traits that affect C (for example, C_3 and C_4 photosynthetic pathways) and N (for example, legumes associated with N-fixing symbionts and non-leguminous species) cycling than have species-poor communities[7,10], and therefore have potentially greater responsiveness of ecosystem functions to elevated CO_2 and N deposition. This can occur because diverse assemblages have a greater likelihood of containing species with strong responses to resources and strong impacts on ecosystem processes compared with species-poor assemblages (that is, a sampling effect)[27,28]. Alternatively, this can occur because the greater range of traits extant in diverse assemblages positively affects competitive associations and interactions (such as niche complementarity and positive species interactions)[3,7,10,28].

Testing the influence of plant diversity on the impacts of elevated CO_2 and N to ecosystem functioning requires simultaneous manipulation of plant species composition, CO_2, and N. Although there have been glasshouse studies[8] of species responses to elevated CO_2 in monocultures versus mixtures, and field studies of monocultures and bi-species mixtures[9,15], this is the first field study, to our knowledge, to test the hypothesis[7] that plant species diversity influences ecosystem-scale biomass responses to elevated CO_2 and N levels. The BioCON experimental facility (see Methods) in Minnesota, USA, was designed expressly for the simultaneous manipulation of these three factors in experimental grassland plots under field conditions, using a well-replicated split-plot experiment comprising a full factorial combination of treatment levels in a completely randomized design.

Our study includes 296 individual plots (each 2×2 m) distributed among six 20-m diameter experimental areas (rings). In three elevated CO_2 rings, a free-air CO_2 enrichment system[29] was used during the 1998 and 1999 growing seasons to maintain the CO_2 concentration at an average of 560 μmol mol^{-1}, a concentration likely to be reached this century[1,2,6]. Three ambient rings (368 μmol mol^{-1} CO_2) were treated identically but without additional CO_2. All plots were planted with 1, 4, 9 or 16 perennial grassland plant species randomly chosen from 16 species in 4 functional groups (C_3 grasses, C_4 grasses, C_3 legumes, C_3 non-legume forbs). Hence high-diversity treatments incorporate greater species and functional group diversity. Native and secondary grasslands in Minnesota typically contain a mixture of these four functional types. Beginning in 1998, half the plots received additional N equivalent to 4 g N m^{-2} yr^{-1}, which is comparable to high rates of N deposition observed in industrialized regions[1].

Diversity, CO_2 and N treatments had significant main effects on total biomass (Table 1, Fig. 1). Above-ground and below-ground biomass both increased markedly with increasing species diversity. Elevated CO_2 predominantly stimulated below-ground biomass, whereas enriched N largely increased above-ground biomass (Table 1). Elevated CO_2 decreased and enriched N increased plant N concentration, total plant N, soil net N mineralization and soil solution N pools (Table 1).

There was no significant interaction between CO_2 and N, and elevated levels of both resources increased total biomass by 27% on average compared with ambient plots (Fig. 1). In essence, the productivity response to elevated CO_2 was not constrained by N limitation in unfertilized plots, even those lacking N-fixing legumes (data not shown). This result differs from many earlier studies[11,18,20], perhaps because we added smaller amounts of N (4 g N m^{-2} yr^{-1}) to represent elevated N deposition, whereas other studies (such as ref. 18) added high amounts (up to 56 g N m^{-2} yr^{-1}) to mimic agricultural N addition.

Although we did not detect a CO_2 and N interaction, there were significant biomass interactions between diversity and CO_2 as well as between diversity and N (Fig. 1; and Methods), largely owing to responses of below-ground biomass, which comprised three-quarters of the total biomass. As the response to elevated CO_2 and N varied among diversity treatments, we tested their effects within diversity levels, using post-hoc comparisons of the mean responses averaged over all four harvests. In the 16-species plots, all treatments

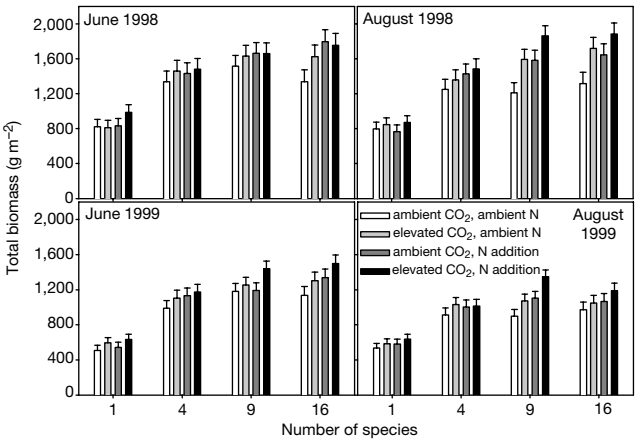

Figure 1 Total biomass (above-ground plus below-ground, 0–20 cm depth) (± 1 s.e.) for plots planted with either 1, 4, 9 or 16 species, grown at four combinations of ambient (368 μmol mol^{-1}) and elevated (560 μmol mol^{-1}) concentrations of CO_2, and ambient N and N addition (4 g N m^{-2} yr^{-1}). Biomass data are shown for each of four harvests (June and August in both 1998 and 1999). The biomass (total and/or below-ground) response to elevated CO_2, enriched N, or both, differed significantly among diversity treatments at every harvest.

Table 1 Average two-year responses of experimental grassland communities to elevated atmospheric CO_2 concentrations, N deposition, and species diversity

Parameter	R^2	F ratio	CO_2 % change	N % change	Species diversity % change
Total biomass	0.54	16.9	+12**	+13***	+98***
Above-ground biomass	0.39	9.2	+8	+23***	+81***
Below-ground biomass	0.50	15.0	+14*	+9*	+105***
Whole plant %N	0.29	5.9	–13***	+14***	–26***
Total plant N content	0.47	12.9	–2	+29***	+64***
Soil net N mineralization	0.23	4.2	–15	+64*	–68***
Soil solution N (0–20 cm)	0.21	3.9	–14	+36	–76**

R^2 and F ratio shown for the whole model (see Methods), for which P values were always less than 0.001. Main effects (% difference, pooled across all other treatments) and significant level (‡, $P < 0.1$; *, $P < 0.05$; **, $P < 0.01$; ***, $P < 0.001$) shown are based on measurements in all 296 plots. Species diversity % effects shown compare 16-species versus 1-species plots.

with elevated levels of either CO_2 or N had significantly greater biomass than the ambient CO_2/ambient N plots. In the 9-species plots, only the elevated CO_2/elevated N treatment had significantly greater biomass than the ambient/ambient treatment. In contrast, there was no significant effect of CO_2 or N treatment, alone or in combination, on total biomass for either the 1- or 4-species levels.

Thus, across the four harvests in 1998 and 1999, the enhancement of biomass owing to either elevated CO_2 or enriched N decreased with declining diversity. In the unamended N treatment, the average stimulation of total biomass in response to elevated CO_2 was 22% in 16-species plots, 18% in 9-species plots, 10% in 4-species plots and 7% in monoculture plots (Fig. 2). Differences in plant species diversity accounted for a fivefold difference in the impacts of CO_2 fertilization on biomass accumulation. For example, whereas elevated CO_2 increased biomass by 258 g m^{-2} on average in the most diverse (16-species) plots, it increased biomass by only 47 g m^{-2} on average in the monocultures (Fig. 2).

Similarly, under ambient CO_2, the average enhancement of total biomass in response to N addition ranged from 25% in 16-species plots to 18%, 11% and 2% in 9-species, 4-species and monoculture plots, respectively (Fig. 2). Thus, biomass enhancement by N enrichment was much less in low-diversity plots—N deposition increased biomass by almost 300 g m^{-2} in the diverse plots and by only 15 g m^{-2} in the monocultures. For plots subjected to both elevated CO_2 and enriched N, biomass increased by more than 400 g m^{-2} in both the 16- and 9-species plots (+35%), but only by roughly 100–150 g m^{-2} in 4-species plots (+15%) and monocultures (+17%).

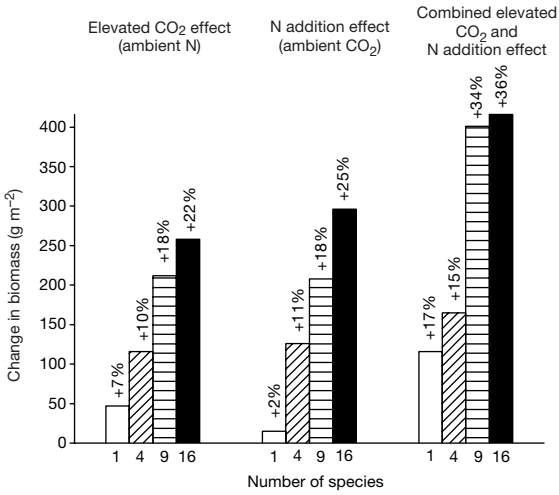

Figure 2 Change in total (above-ground plus 0–20 cm below-ground) biomass (compared with ambient levels of both CO_2 and N) in response to elevated CO_2 alone (at ambient soil N), to enriched N alone (at ambient CO_2), and to the combination of elevated CO_2 and enriched soil N, for plots containing 1, 4, 9 or 16 species. Data were averaged for 4 harvests over 2 yr. Per cent change is shown above each histogram for each diversity treatment.

By sorting above-ground biomass to species, we found that the increase in biomass with increased diversity at each resource level was due largely to the four species that were most abundant in mixtures. The four species *Achillea*, *Bromus*, *Lupinus* and *Poa* together made up more than 80% of the above-ground biomass in 16-species plots (Table 2) and represent all three of the C_3 functional groups. Three of these species were among the four most productive species in monocultures. However, all four of the species abundant in mixtures had lower average monoculture biomass at a given resource level than the average 16-species mixtures at the same resource level (Table 2) and no one species comprised more than one-third of the above-ground biomass in the 16-species mixture at any level. Thus, consistent with a multiple-species 'sampling effect', there was collective dominance in 16-species mixtures by three of the more productive members of the species pool, but this dominance was moderate, and other species also contributed to the greater biomass of the high-diversity plots.

The effects of species diversity on biomass accumulation responses to elevated CO_2 and N deposition also appear to result from the combination of multiple-species sampling effects and niche complementarity or positive species interactions. The four dominant species (*Achillea*, *Bromus*, *Lupinus* and *Poa*) were responsible for much of the increase in biomass in 16-species plots at elevated resource levels (that is, elevated CO_2, enriched N, or both) and showed large responses to these treatments when grown in monoculture (Table 2; for example, *Achillea* and *Lupinus* for elevated CO_2; *Poa* and *Bromus* for elevated N).

Although the response of *Poa* monocultures to N fertilization was large enough to suggest that it may have the capability of explaining most of the increased biomass response of the 16-species mixture if heavily dominant, *Poa* was not more than one-third of the total above-ground biomass in those mixtures, indicating that other species are also important. For elevated CO_2 at ambient N, the stimulation of total biomass (+258 g m^{-2}) in 16-species mixtures was greater than the stimulation in monoculture of any species to elevated CO_2. Thus, the increase in biomass of 16-species plots with increasing resource supply was substantially due to the presence and response of species that do respond strongly in monocultures (that is, interpretable as mainly a sampling effect), but they collectively increased more when together than when in monoculture (a niche effect).

In addition, different species were responsible for the enhanced responses to different combinations of CO_2 and N, again suggesting niche differentiation. The increased total biomass response of 16-species plots to elevated CO_2 at ambient N (of +22%, Figs 1 and 2) was largely due to the response of *Achillea*, *Lupinus* and *Bromus*, each of which maintained a roughly similar fraction of a higher total above-ground biomass under elevated than ambient CO_2 (Table 2). At either ambient or elevated CO_2, the enhanced biomass in N-enriched 16-species plots as compared with ambient/ambient plots was due to increases in biomass by *Poa*, *Bromus* and *Achillea*, in that

Table 2 Total biomass of 16-species mixtures and of monocultures of the dominant species in the 16-species mixtures

	Ambient CO_2, ambient N		+CO_2, ambient N		Ambient CO_2, +N		+CO_2, +N	
Biomass (g m^{-2}) of 16-species mixtures	1,165		1,423		1,462		1,581	
Species	Monoculture biomass (g m^{-2})	% of 16-species mixture	Monoculture biomass (g m^{-2})	% of 16-species mixture	Monoculture biomass (g m^{-2})	% of 16-species mixture	Monoculture biomass (g m^{-2})	% of 16-species mixture
Achillea	1,124	34%	1,314	33%	848	31%	1,321	34%
Poa	979	22%	1,089	19%	1,322	33%	1,407	27%
Lupinus	509	15%	672	17%	449	6%	670	9%
Bromus	1,021	11%	989	12%	1,228	14%	1,082	14%
All other species	590	18%	615	19%	587	16%	664	16%

Totals are above-ground plus below-ground biomass, at all four combinations of CO_2 and N. Also shown is the % of total above-ground biomass for each of the dominant species in the 16-species mixtures at each CO_2 and N combination.

order, despite a decline in *Lupinus* biomass.

These results suggest that multiple-species sampling effects, niche complementarity and positive species interactions[3,7,10,28] jointly help to explain the greater responses of diverse than species-poor plots to elevated levels of the two major global change factors: atmospheric CO_2 and N deposition. Moreover, the central finding of this study—that changes in plant diversity influence the magnitude of CO_2 and N impacts on ecosystem functioning—is important regardless of which set of mechanisms are operating.

Our study raises concerns about the consequences of widespread changes in plant composition and diversity in ecosystems worldwide for responses to other global changes[1,2], because the results show that, in response to elevated levels of CO_2 and N, ecosystems with decreased diversity may acquire less C and biomass than ecosystems with greater diversity. It is unclear whether the responses observed in 1998–1999 will change with time as the composition of the communities changes, the climate varies, and long-term soil microbial feedbacks occur[20–25], or whether natural or managed vegetation would respond similarly to combinations of diversity, CO_2 and N. Nonetheless, our results suggest that the reduction of diversity occurring globally may reduce the capacity of ecosystems to capture additional C under conditions of rising atmospheric CO_2 concentrations and N deposition levels. □

Methods

BioCON experiment

The BioCON (Biodiversity, CO_2 and N) experiment (http://swan.lter.umn.edu/biocon/) is located at the Cedar Creek Natural History area in Minnesota, USA. Plots were established on a secondary successional grassland on a sandy outwash soil after removing the previous vegetation. The experimental treatments were arranged in complete factorial combination of CO_2 (ambient or 560 μmol mol^{-1}), species number (1, 4, 9, and 16) and N level (control and fertilized). The species numbers were chosen as the squares of 1, 2, 3 and 4 to represent roughly equal effective differences in diversity, on the basis of earlier studies[4]. Each plot was planted in 1997 with 12 g m^{-2} of seed partitioned equally among all species planted in a plot.

The design consisted of a split-plot arrangement of treatments in a completely randomized design. CO_2 treatment is the whole-plot factor and is replicated three times among the six rings. The subplot factors of species number and N treatment were assigned randomly and replicated in individual plots among the six rings. For each of the four combinations of CO_2 and N levels, pooled across all rings, there were 32 randomly assigned replicates for the plots planted to 1 species, 15 for those planted to 4 species, 15 for 9 species, and 12 for 16 species. Beginning in 1998, the plots assigned to the N addition treatment were amended with 4 g N m^{-2} yr^{-1}, applied over three dates each year. CO_2 was added in elevated treatments during all daylight hours from 9 April to 16 October 1998, and from 20 April to 9 November 1999. Although there was modest variation in CO_2 concentrations spatially within and across rings, the average CO_2 concentrations were not more than 1–2 μmol mol^{-1} different among rings, or among diversity or N treatment levels averaged within and across rings (see Supplementary Information).

Species and biomass measurements

The 16 species used in this study were all native or naturalized to the Cedar Creek Natural History Area. They include four C_4 grasses (*Andropogon gerardii*, *Bouteloua gracilis*, *Schizachyrium scoparium*, *Sorghastrum nutans*), four C_3 grasses (*Agropyron repens*, *Bromus inermis*, *Koeleria cristata*, *Poa pratensis*), four N-fixing legumes (*Amorpha canescens*, *Lespedeza capitata*, *Lupinus perennis*, *Petalostemum villosum*) and four non-N-fixing herbaceous species (*Achillea millefolium*, *Anemone cylindrica*, *Asclepias tuberosa*, *Solidago rigida*), and all are referred to by genus elsewhere. Monocultures of all species were replicated twice at all CO_2 and N levels. The 4- and 9-species plots were random selections from all species. Plots were regularly weeded to remove unwanted species. In June and August of each year, we assessed above- and below-ground (0–20 cm) biomass, plant C and N, and soil N (see Supplementary Information). Soil net N mineralization rates were measured once each year. Above-ground biomass was sorted to species at each harvest. The species richness of clipped above-ground biomass samples was 1.0, 3.8, 8.0 and 13.6 species on average for plots planted with 1, 4, 9 and 16 species, respectively, on the basis of the number of species identified in each plot from the four above-ground harvests (each 0.1 m^2).

Statistical analysis

In analysis of variance all treatment effects were considered fixed. Using *F*-tests, the effect of CO_2 (1 degree of freedom, d.f.) was tested against the random effect of ring nested within CO_2 (4 d.f.). The main effects of species number (3 d.f.) and N (1 d.f.), and interactions between CO_2 and N were tested against the residual error. The main effect of species number and its first-order interaction terms were partitioned into single-degree-of-freedom contrasts for linear, quadratic and cubic terms to test for interactions between diversity and either CO_2 or N treatments, and additionally to test hypotheses about predetermined contrasts of elevated resource levels (elevated CO_2, enriched N, or both) versus the ambient/ambient conditions. There were interactions for below-ground biomass between species diversity and CO_2 treatments in the August 1998 ($P < 0.05$), June 1999 ($P < 0.10$) and August 1999 ($P < 0.10$) harvests, and between species diversity and N treatments in the June 1999 ($P < 0.05$) and August 1999 ($P < 0.05$) harvests. For the pre-planned contrast between the ambient/ambient and the elevated CO_2/enriched N treatments, there were significantly different responses (for below-ground and total biomass) for different diversity treatments at the June 1998 ($P < 0.05$), August 1998 ($P < 0.05$) and June 1999 ($P < 0.05$) harvests. Given interactions between species diversity and resource treatments, post-hoc Student's *t*-tests were also conducted to compare individual resource treatments within species diversity levels. All analyses were conducted for each harvest, for each year (pooling harvest data by plot), and across years averaged (pooling data for all harvests by plot), with similar results, although there was harvest-to-harvest variation (see Fig. 1).

Received 20 November 2000; accepted 18 January 2001.

1. Vitousek, P. M. Beyond global warming: ecology and global change. *Ecology* **75,** 1861–1876 (1994).
2. Sala, O. E. *et al.* Global biodiversity scenarios for the year 2100. *Science* **287,** 1770 (2000).
3. Hector, A. *et al.* Plant diversity and productivity experiments in European grasslands. *Science* **286,** 1123 (1999).
4. Tilman, D. *et al.* The influence of functional diversity and composition on ecosystem processes. *Science* **277,** 1300–1302 (1997).
5. Stocker, R., Körner, C., Schmid, B., Niklaus, P. A. & Leadley, P. W. A field study of the effects of elevated CO_2 and plant species diversity on ecosystem-level gas exchange in a planted calcareous grassland. *Global Change Biol.* **5,** 95–105 (1999).
6. Schimel, D. *et al.* Contribution of increasing CO_2 and climate to carbon storage by ecosystems in the United States. *Science* **287,** 2004 (2000).
7. Bolker, B. M., Pacala, S. W., Bazzaz, F. A., Canham, C. D. & Levin, S. A. Species diversity and ecosystem response to carbon dioxide fertilization: conclusions from a temperate forest model. *Global Change Biol.* **1,** 373 (1995).
8. Navas, M.-L., Garnier, E., Austin, M. P. & Gifford, R. M. Effect of competition on the responses of grasses and legumes to elevated atmospheric CO_2 along a nitrogen gradient: differences between isolated plants, monocultures and multi-species mixtures. *New Phytol.* **143,** 323–331 (1999).
9. Schenk, U., Jäger, H.-J. & Weigel, H.-J. The response of perennial ryegrass/white clover swards to elevated atmospheric CO_2 concentrations. *New Phytol.* **135,** 67–79 (1997).
10. Schmid, B., Joshi, J., Schlapfer, F. in *Functional Consequences of Biodiversity: Experimental Progress and Theoretical Extensions* (eds Kinzig, A., Tilman, D. & Pacala, S.) (Princeton Univ. Press, Princeton, in the press).
11. Körner, C. & Bazzaz, F. A. *Carbon Dioxide, Populations and Communities* (Academic, San Diego, 1996).
12. DeLucia, E. H. *et al.* Net primary production of a forest ecosystem with experimental CO_2 enrichment. *Science* **284,** 1177–1179 (1998).
13. Wand, S. J., Midgley, G. F., Jones, M. H. & Curtis, P. S. Responses of wild C4 and C3 (Poaceae) species to elevated atmospheric CO_2 concentration: a meta-analytic test of current theories and perceptions. *Global Change Biol.* **5,** 723–741 (1999).
14. Owensby, C. E., Ham, J. M., Knapp, A. K. & Auen, L. M. Biomass production and species composition change in a tallgrass prairie ecosystem after long-term exposure to elevated atmospheric CO_2. *Global Change Biol.* **5,** 497–506 (1999).
15. Lüscher, A., Hendrey, G. R. & Nösberger, J. Long-term responsiveness to free-air CO_2 enrichment of functional types, species, and genotypes of plants from fertile permanent grassland. *Oecologia* **113,** 37–45 (1998).
16. Warwick, K. R., Taylor, G. & Blum, H. Biomass and compositional changes occur in chalk grassland turves exposed to elevated CO_2 for two seasons in FACE. *Global Change Biol.* **4,** 375–385 (1998).
17. Leadley, P. W., Niklaus, P. A., Stocker, R. & Körner, C. A field study of the effects of elevated CO_2 on plant biomass and community structure in a calcareous grassland. *Oecologia* **118,** 39–49 (1999).
18. Zanetti, S. *et al.* Does nitrogen nutrition restrict the CO_2 response of fertile grassland lacking legumes? *Oecologia* **112,** 17–25 (1997).
19. Hebeisen, T. *et al.* Growth response of *Trifolium repens* L. and *Lolium perenne* L. as monocultures and bi-species mixture to free air CO_2 enrichment and management. *Global Change Biol.* **3,** 149–160 (1997).
20. Zak, D. R. *et al.* Atmospheric CO_2, soil-N availability, and allocation of biomass and nitrogen by *Populus tremuloides*. *Ecol. Appl.* **10,** 34–46 (2000).
21. Hu, S., Firestone, M. K., Chapin, F. S. III. Soil microbial feedbacks to atmospheric CO_2 enrichment. *Trends Ecol. Evol.* **14,** 433 (1999).
22. Diaz, S., Grime, J. P., Harris, J. & McPherson, E. Evidence of a feedback mechanism limiting plant response to elevated carbon dioxide. *Nature* **364,** 616–617 (1993).
23. Zak, D. R. *et al.* Elevated atmospheric CO_2 and feedback between carbon and nitrogen cycles. *Plant Soil* **151,** 105–117 (1993).
24. Hungate, B. A. *et al.* The fate of carbon in grasslands under carbon dioxide enrichment. *Nature* **388,** 576–579 (1997).
25. Cannell, M. & Thornley, J. N-poor ecosystems may respond more to elevated [CO_2] than N-rich ones in the long term. A model analysis of grassland. *Global Change Biol.* **4,** 431–442 (1998).
26. Vitousek, P. M. & Howarth, R. W. Nitrogen limitation on land and in the sea: how can it occur? *Biogeochemistry* **13,** 87–115 (1991).
27. Huston, M. A. Hidden treatments in ecological experiments: re-evaluating the ecosystem function of biodiversity. *Oecologia* **110,** 449–460 (1997).
28. Tilman, D., Lehman, C. L. & Thomson, K. T. Plant diversity and ecosystem productivity: theoretical considerations. *Proc. Natl Acad. Sci. USA* **94,** 1857–1861 (1997).
29. Lewin, K. F., Hendrey, G. R., Nagy, J. & LaMorte, R. Design and application of a free-air carbon dioxide enrichmnent facility. *Agric. Forest Meteorol.* **70,** 15–29 (1994).

Supplementary information is available on *Nature*'s World-Wide Web site (http://www.nature.com) or as paper copy from the London editorial office of *Nature*.

Correspondence and requests for materials should be addressed to P.R. (e-mail: preich@forestry.umn.edu).

insight overview

Enabling the chemistry of life

Christopher Walsh

Biological Chemistry and Molecular Pharmacology Department, Harvard Medical School, Boston, Massachusetts 02115, USA

Enzymes are the subset of proteins that catalyse the chemistry of life, transforming both macromolecular substrates and small molecules. The precise three-dimensional architecture of enzymes permits almost unerring selectivity in physical and chemical steps to impose remarkable rate accelerations and specificity in product-determining reactions. Many enzymes are members of families that carry out related chemical transformations and offer opportunities for directed *in vitro* evolution, to tailor catalytic properties to particular functions.

The myriad chemical transformations carried out by every living organism are enabled by hundreds to thousands of proteins (enzymes) and, less frequently, RNAs (ribozymes), which have catalytic activity for conversion of a particular set of substrates to specific products. Some of these reactions are carried out by related families of protein biocatalysts, which act generically in the same way but exert specific recognition for transformation of a particular substrate molecule. For example, the orderly control of the location and lifetime of proteins in cells is managed by dozens of related proteases that hydrolyse peptide bonds of protein substrates in ways that are controlled in time and space. Proteases can be exquisitely specific for a particular peptide bond in a protein substrate, or they can be relentlessly nonspecific: the former set of proteases are involved in turning on biological signals, the latter in the clean-up phases of degradation and protein turnover.

When cells respond to external messenger molecules, such as the protein growth factors and hormones erythropoietin and insulin, or small-molecule hormones such as adrenaline or prostaglandins, signalling pathways are set in motion by catalytic action of cascades of protein kinases. The protein kinases are built from a small set of architectural types, and all catalyse phosphoryl transfer from ATP to the side-chain hydroxyl of serine, threonine or tyrosine residues. There are hundreds of such kinases in animal genomes. Selectivity is imposed on this generic chemical phosphorylation reaction by protein–protein interactions between a given kinase and its protein substrate and by cascades of such kinase/protein substrate pairs that ultimately lead to changes in activity and location of proteins, and to selective gene activation.

In addition to the large number of enzymes that act on macromolecular protein substrates, there are also enzymes that engage in truly sophisticated chemistry on small

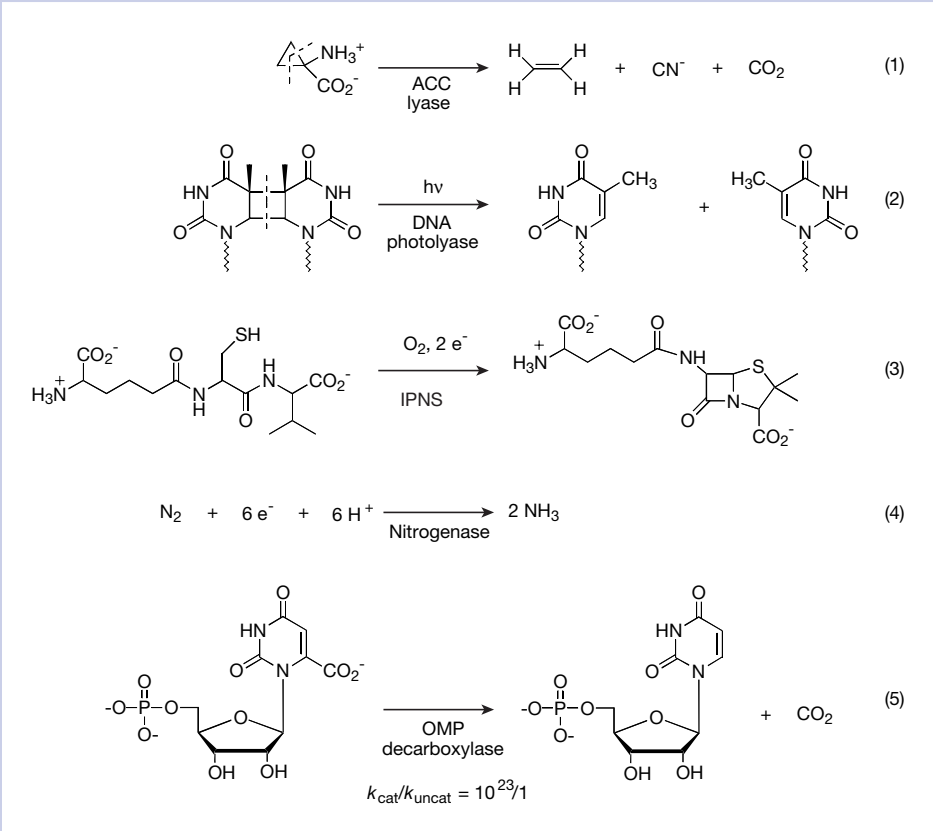

Figure 1 Diverse chemical reactions facilitated by biocatalysts. ACC lyase, 1-aminocyclopropane-1-carboxylate lyase; IPNS, isopenicillin *N* synthase; OMP decarboxylase, orotidine-5′-phosphate decarboxylase.

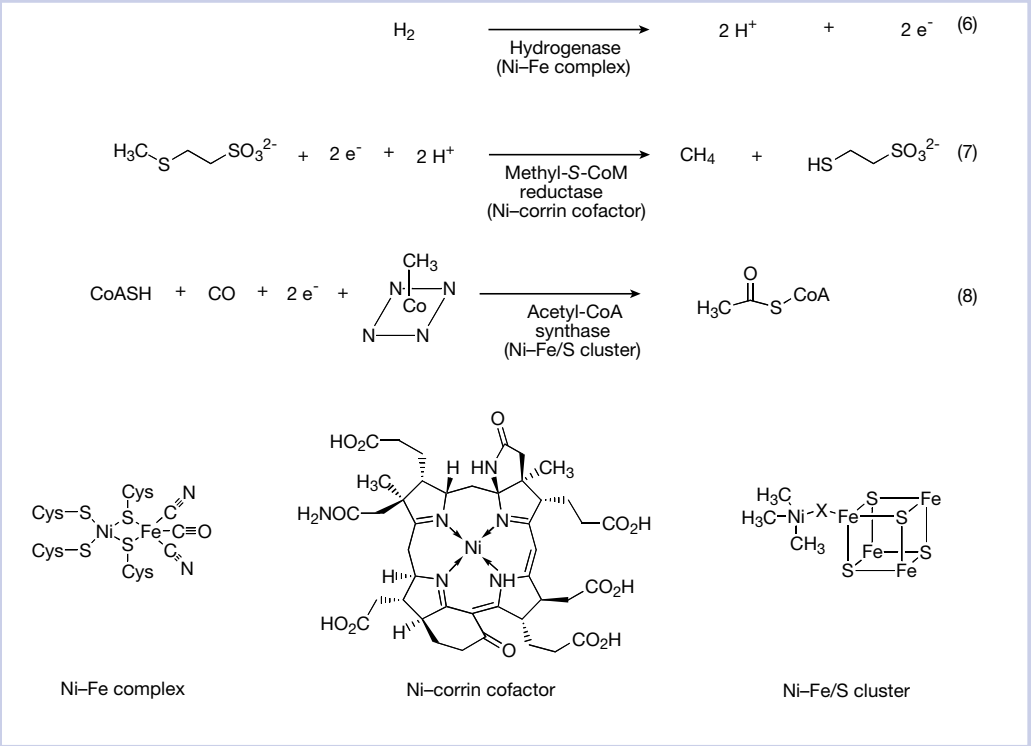

Figure 2 Nickel-based enzymatic transformations in methanogenic archaebacteria.

organic molecules. The fragmentation of 1-aminocyclopropane-1-carboxylate to the fruit-ripening hormone ethylene[1], the photon-induced 2+2 cycloreversion of thymine dimers to repair DNA damaged by ultraviolet light[2], the bis-cyclization of the tripeptide aminoadipoyl-cysteinyl-D-valine (ACV) to isopenicillin *N* (ref. 3), and the reduction of dinitrogen (N_2) to two molecules of ammonia (NH_3) during nitrogen fixation[4] are just a few examples of the range of biological chemistry facilitated by biocatalysts (Fig. 1). Enzymes as biocatalysts are remarkable not only in themselves, but also for the inspiration and guidance they provide to synthetic organic and inorganic chemists striving to reproduce and expand nature's chemical repertoire. Several of the useful attributes of biocatalysts, such as their use as reagents for chemical synthesis and scale-up, and directed evolution to tailor chemical transformations, are explored in other articles in this Insight.

Biocatalysts and their *ex vivo* utility

Biocatalysts carry out the chemistry of life, the controlled chemical transformations in primary metabolism and the generation of natural-product diversity in secondary metabolism of plants and microbes. Classically, the subset of proteins with catalytic activity — the enzymes — has been the focus of biocatalysis research. But there is an increasing focus on catalytic RNA (ribozymes), the discovery of which in the 1980s supported the arguments for an 'RNA world'[5,6] antecedent to the contemporary world where proteins are the workhorse biocatalysts. Most recently, Joyce and co-workers[7] have reported catalytic DNA molecules, and directed evolution of both RNA and DNA biocatalysts will continue to expand their potential. The current set of RNA and DNA catalysts have been assayed and developed for activities in nucleic-acid replication and in protein synthesis[8,9], but it remains to be seen how suitable they will be for the chemically diverse reactions encompassed by existing enzyme catalysts.

The twin hallmarks of enzyme biocatalysts are the remarkable specificities and sometimes phenomenal rate accelerations achieved. A typical enzyme, with a relative molecular mass of 50,000 (M_r 50K), is comprised of 450 amino-acid residues: 19 chiral L-amino acids and glycine. If glycine makes up 10% of the residues, then there are at least 400 residues with chiral centres to provide an asymmetric microenvironment for substrate binding and subsequent chemical transformation in the enzyme's active site. This is the underlying structural basis for the action of all enzymes as chemoselective and regio- and stereospecific catalysts. In terms of rate accelerations, the relative values over nonenzymatic rates of transformation are often 10^{10}, for example for protease-mediated hydrolysis of peptide bonds, and can reach 10^{23} in the example of orotidine decarboxylase in the pyrimidine biosynthetic pathway[10] (reaction 5 in Fig. 1). In absolute terms, enzymes have turnover numbers from as slow as one catalytic event per minute to 10^5 per second (as in the hydration of CO_2 to HCO_3^- by carbonic anhydrase)[11].

These two attributes of enzymatic biocatalysts have spurred much investigation into both the structural and mechanistic bases of the chemical transformations and have stimulated much of the study of enzymes in chemical synthesis (see review in this issue by Koeller and Wong, pages 232–240). *In vivo*, enzymes operate in buffered aqueous environments with ionic strength and pH control, although microbes that live at extremes of temperature and pH are of particular current interest because of the stability of their constituent enzymes. Much attention in biocatalyst process design (see accompanying review by Witholt *et al.*, pages 258–268) is on how to prolong useful lifetimes of enzyme catalysts and to have them operate in media not ordinarily compatible with life.

The past two decades have also witnessed an intense exploration of catalytic antibodies[12]. To prepare these antibodies, ligands are synthesized that typically mimic transition states of particular chemical transformations, such as ester hydrolysis, amide synthetase and Claisen condensation. Monoclonal antibodies are then selected that display high-affinity binding to the ligands, thus enriching for antibody proteins with a binding-site geometry complementary to the shape of the true transition state. Some of the antibodies selected in this way show catalysis of the desired reactions, with the selectivity and rate accelerations expected for chiral protein-based catalysts[13,14]. But low catalytic turnover numbers have so far limited the use of catalytic antibodies in chemical synthesis or process work.

Biocatalysts or biomimetic catalysts?

With their unerring stereoselectivity and high catalytic efficiency, nature's enzymatic catalysts have been a stimulus and counterpoint

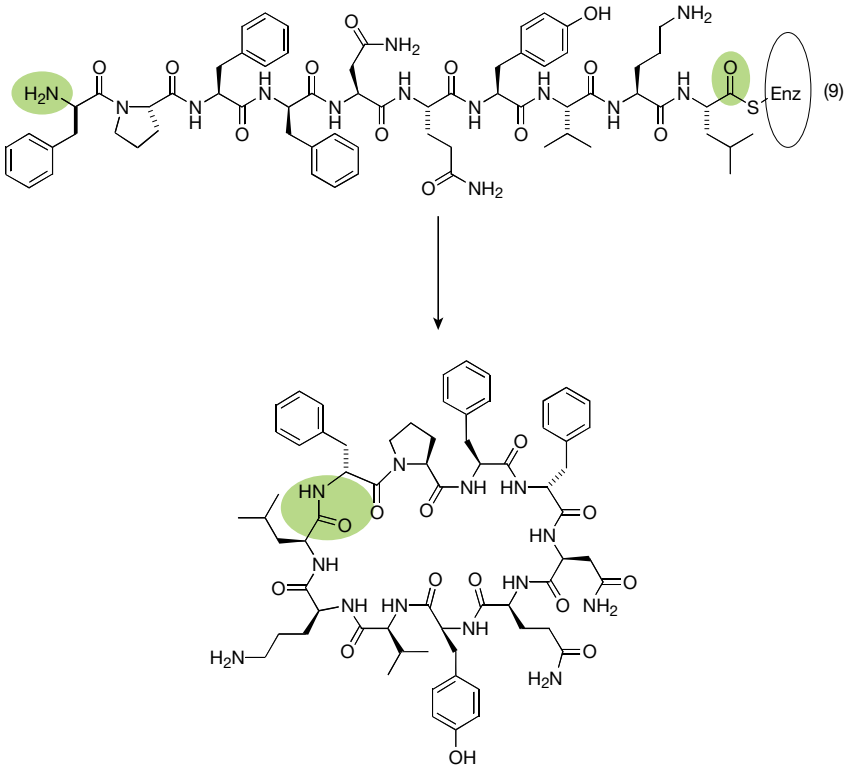

Figure 3 Cyclization catalysed by the thioesterase domain of tyrocidine synthetase.

for generations of chemists who have designed and tested bioorganic and bioinorganic versions of biomimetic catalysts, whether for example to mimic macrocyclizations of natural products or to produce analogues of hydrogenase or nitrogenase catalysts or the photosynthetic splitting of water[15]. The mimics may operate under harsher solvent and temperature conditions, and may be more robust in terms of lifetime (if not throughput per catalyst molecule). When organic coenzymes (such as flavins, pyridoxal or thiamin) or inorganic cofactors (iron/sulphur clusters, metalloporphyrins) are crucial components of the enzymatic catalysis, the biomimetic and natural catalysts often show design convergence and may recapitulate some of the steps in biocatalyst evolution. The three nickel enzymes in methanogenic bacteria (thought to be contemporary descendants of primordial organisms), which carry out nickel-based hydrogenation, nickel-based methyl thioether reduction to methane, and nickel-based carbonylation of a methyl co-substrate to produce acetate, can be viewed as such an intersection[16,17] (Fig. 2).

When is it worthwhile for the synthetic or process chemists to reject synthetic reagents and catalysts in favour of enzymes to carry out a specific transformation? This may vary with individual preference and each case must be judged on its own merits. Lipases and other hydrolases have clear advantages in kinetic resolutions of intermediates (see below), penicillin acylases have long been a mainstay of semisynthetic processes in the β-lactam antibiotic industry, and enzymatic aldol condensations have shown their worth in complex oligosaccharide syntheses[18].

Chemical transformations well suited to enzymes

The accompanying review by Khosla and Harbury (pages 247–252) explores the multimodular enzymes that function as molecular solid-state assembly lines for the generation of thousands of polyketide natural products and non-ribosomal peptide antibiotics, including important medicinal compounds such as erythromycin, rapamycin, epothilone, lovastatin, penicillins, cyclosporin and vancomycin[19–21]. These sequentially elongating acyl transfers seem particularly apt loci for use as enzymatic rather than biomimetic catalysis. Some of the assembly lines, such as those for erythromycin or cyclosporin, produce the intramolecularly cyclized macrolactones or macrolactams. It has recently been shown[22] that the last 30K (thioesterase) domain of the 724K protein assembly line of tyrocidine synthetase retains the ability to cyclize 9–11-residue peptidyl thioesters with regio- and stereoselectivity, raising the prospect for practical enzymatic macrocyclizations by a robust, small protein fragment (Fig. 3, reaction 9).

The reprogramming of the component enzyme domains of these assembly lines to create new, unnatural 'natural' products is one of the goals of combinatorial biosynthesis. The order of the enzymatic domains in the assembly lines specifies which monomer substrates are activated, condensed and elongated. So altering the order and permutations of these domains offers the chance to control product structure. The directed evolution of the catalytic domains of polyketide synthase (PKS) and non-ribosomal peptide synthetase (NRPS) assembly lines by gene shuffling and other approaches (see accompanying review by Arnold, pages 253–257) can create designed diversity in complex natural products.

Once the nascent products have been released from the PKS and NRPS assembly lines, the polyketide or polypeptide may require further enzymatic transformations to attain antibiotic properties. This is the case for penicillins, vancomycin and erythromycin, to cite just three important examples[19]. Baldwin and co-workers[23,24] showed that the tripeptide ACV is oxidatively transformed to the 4-5 bicyclic β-lactam ring system by isopenicillin *N* synthase (IPNS; Fig. 1, reaction 3). IPNS is a member of a substantial family of iron-containing enzymes that use Fe^{2+} to activate both O_2 and the specific co-substrate for complex redox chemistry[25]. In IPNS, both atoms of dioxygen are reduced to water and the ACV tripeptide undergoes four-electron oxidation and directed C–S bond and C–C bond formation as the β-lactam forms. A cousin of IPNS, the expandase enzyme, is used by cephalosporin-producing organisms to expand the five-membered ring in penicillins to the six-membered ring in cephalosporin

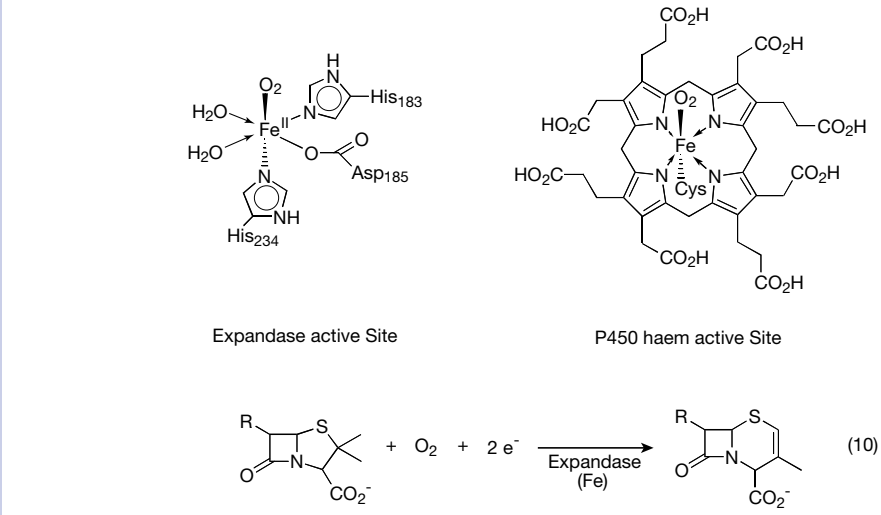

Figure 4 Comparison of expandase active site with a typical haemprotein oxygenase.

antibiotics (Fig. 4, reaction 10). The ligand set around the active-site iron — one Glu, two His residues — is the same, but the reaction flux is distinct (Fig. 4). Other members of this non-haem dioxygenase family include the enzyme responsible for hydroxylating prolyl residues in protocollagen to predispose it to triple-helix formation in mature collagen, the most abundant protein in the human body. There are clear potential benefits to understanding the molecular basis for how the high-valent oxo-iron reagents are controlled and directed to flawlessly different chemical outcomes in the members of this redox enzyme family, so that they might be subjected to *in vitro* evolution to generate new reaction fluxes.

Many natural products, from morphine and codeine to vancomycin, undergo oxidative cyclization reactions that are regio- and stereospecific and seem to be mediated by a different superfamily of iron-containing oxidases, the cytochromes P450, with Fe^{2+} embedded in a haem macrocycle (Fig, 4). Protein superfamilies are groups of proteins with distinct chemical functions, amino-acid sequences of recognizable but sometimes marginal homology, and convergent three-dimensional structures. In the vancomycin family of glycopeptide antibiotics there are three crosslinks that convert an acyclic heptapeptide, the product of the NRPS assembly line, into a rigid scaffold, crosslinked at Tyr_2-$PheGly_4$-Tyr_6 and $PheGly_5$-dihydroxy$PheGly_7$ (Fig. 5, reaction 11). There are three P450 cytochromes in the biosynthetic gene cluster; each might enact a regiospecific phenolic crosslink. Harnessing such catalysts for related transformations might lead to new vancomycins.

Several natural products contain tandem five-membered-ring heterocycles (oxazoles and thiazoles) that arise from enzymatic cyclization of serine or cysteine residues in peptide precursors[26]. These include the *Escherichia coli* antibiotic microcin B17, which kills neighbouring bacteria by poisoning the enzyme DNA gyrase and thus blocking DNA replication, in much the same way as does the best-selling antibiotic ciprofloxacin[27] (Fig. 6). Such heterocycles are also found in the iron-chelating siderophores that act as virulence factors in infections by *Pseudomonas aeruginosa*, *Vibrio cholerae* and the causative agent of the black plague, *Yersinia pestis*[28,29]. Enzymes that heterocyclize serine, threonine and cysteine side chains in peptides (Fig. 6, reactions 12, 13) may create either DNA-seeking or iron-chelating sites in any peptide library that could then be screened for biological activity.

Superfamilies, genomics and enzyme evolution

The iron-containing dioxygenases that include IPNS and expandase, and the cytochrome P450 variants that introduce crosslinks, comprise redox enzyme superfamilies that are good candidates for engineering for altered catalytic properties and specificities. Genomic and proteomic searches can identify many enzyme superfamily members through amino-acid sequence homologies, in which scaffolding and structural architecture will be predictable. Some of these proteins are of unknown ('orphan') function, and the assignment of function is one of the major postgenomic challenges of proteomic research. Recent cases in the crotonase superfamily (Fig. 7, reactions 14–16) and enolase superfamily (Fig. 7, reactions 17–19)[30–32] indicate that the active sites all generate carbanionic transition states from bound substrates and then use carbanion chemistry for directed fluxes and distinct product outcomes. These families should be fruitful starting points for directed enzyme evolution to elicit new fluxes, based on the knowledge that carbanion chemistry will be facilitated

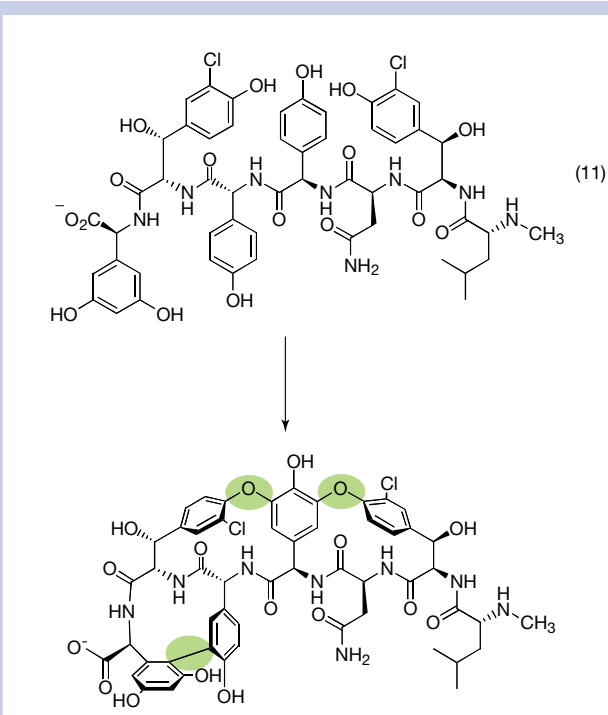

Figure 5 Crosslinking by cytochrome P450 enzymes to produce the vancomycin Aglycone.

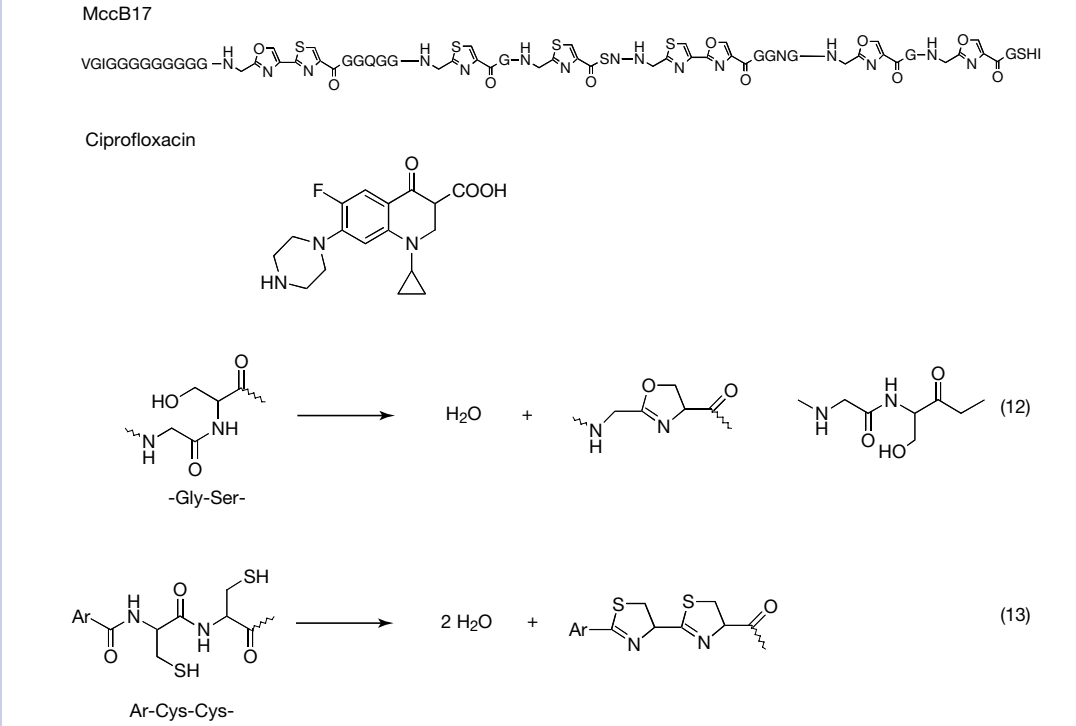

Figure 6 DNA gyrase inhibitors and biosynthesis of peptide heterocycles.

in one of the co-substrates and that binding sites can be re-engineered for electrophilic substrate components.

Once an enzyme has been evolved to have a detectable and desirable new activity[33], additional rounds of *in vitro* evolution can improve its stability and robustness. The biological selection methods are sufficiently powerful that one can find outcomes that are very rare biologically in a short space of time. A good example is the recent report[34] of expression of a functional carotenoid biosynthetic pathway in *E. coli* by selecting for bacteria that become red. The continuing progress in biological production of polyhydroxyalkanoate polymers with controlled sizes and properties[35] by engineering the respective polymerases increases the likelihood of economically viable production of these biodegradable plastics by biocatalysis.

Enzymes in bioremediation

One of the most active areas of applied enzymology in the past two decades has been the study of enzymes capable of bioremediation: the breakdown of organic and inorganic pollutants. There are now substantial databases of enzymes and the bioremedial transformations[36] they catalyse, which include the breakdown of aromatic and heteroaromatic pollutants by oxidative, reductive and hydrolytic transformations. Iron-containing dioxygenases and monooxygenases, with overlapping regio- and chemospecificities, are superfamilies that represent good starting points for application of many of the strategies noted here and in the specific accompanying articles for directed enzyme evolution to broaden substrate recognition. It is likely that bioremediation scenarios in the field will require the tailored enzymes to work in their host microbial cells rather than as *ex vivo* catalysts. Engineering of multistep metabolic pathways by introducing heterologous genes[37] and *in vivo* expression may well be required for efficient degradation of non-biogenic compounds. As many waste sites have a witches' brew of foreign compounds, multiple pathways engineered stably into a microbe or, more probably, mixed bacterial communities that can coexist stably, will be required. The enzymology of processing of toxic inorganic ions has also progressed in recent years to include mercury, copper, cadmium, silver, arsenic and cobalt. This might ultimately make remediation schemes for inorganic pollutants feasible[38].

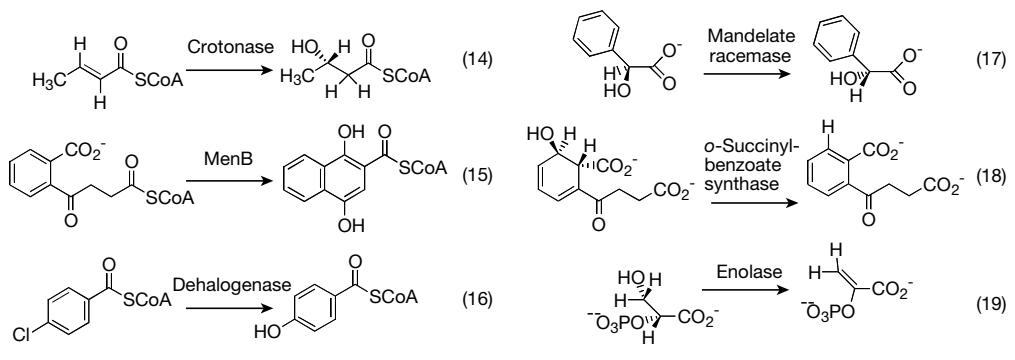

Figure 7 Representative reactions catalysed by the crotonase superfamily and the enolase superfamily.

Conclusions

As structural genomics continues to reveal the folds and scaffolds of several members of all the principal superfamilies of enzymes, the molecular bases of recognition of substrates and directed fluxes through specific transition states to particular subsets of products will become increasingly clarified. In turn this will aid in enzyme evolution to select and detect new activities and then to incorporate improved catalytic efficiency, attributes of specificity, and structural features optimized to a given operating microenvironment. For both *in vitro* applications for a specific synthetic chemical step and for *in vivo* construction of new metabolic pathways, the applications for enzymes in practical biocatalysis will continue to burgeon. Small-molecule chemical transformation catalysed by enzymes from microorganisms that live in unusual environments or conduct chemical warfare against their neighbours have been and are likely to remain good hunting grounds for new enzyme transformations. □

1. Peiser, G. *et al.* Formation of cyanide from carbon 1 of 1-aminocyclopropane-1-carboxylic acid during its conversion to ethylene. *Proc. Natl Acad. Sci. USA* **81,** 3059–3063 (1984).
2. Sancar, A. Structure and function of DNA photolyase. *Biochemistry* **33,** 2–9 (1994).
3. Schofield, C. J. *et al.* Proteins of the penicillin biosynthesis pathway. *Curr. Opin. Struct. Biol.* **7,** 857–864 (1997).
4. Bertino, I., Gray, H. B., Lippard, S. J. & Valentine, J. S. *Bioinorganic Chemistry* (University Science Books, Mill Valley, CA, 1994).
5. Gesteland, R., Atkins, J. & Cech, T. R. (eds) *The RNA World* 2nd edn (Cold Spring Harbor Laboratory Press, 1999).
6. Narlikar, G. J. & Herschlag, D. Mechanistic aspects of enzymatic catalysis: lessons from comparison of RNA and protein enzymes. *Annu. Rev. Biochem.* **66,** 19–59 (1997).
7. Sheppard, T. L., Ordoukhanian, P. & Joyce, G. F. A DNA enzyme with N-glycosylase activity. *Proc. Natl Acad. Sci.* **97,** 7802–7807 (2000).
8. Zhang, B. & Cech, T. R. Peptide bond formation by *in vitro* selected ribozyme. *Nature* **390,** 96–100 (1997).
9. Cech, T. R. & Golden, B. L. in *The RNA World* 2nd edn (eds Gesteland, R., Atkins, J. & Cech, T. R.) 321–349 (Cold Spring Harbor Laboratory Press, 1999).
10. Radzicka, A. & Wolfenden, R. A proficient enzyme. *Science* **267,** 90–93 (1995).
11. Stryer, L. *Biochemistry* 4th edn (Freeman, San Francisco, 1995).
12. Patten, P. A. *et al.* The immunological evolution of catalysis. *Science* **271,** 1086–1091 (1996).
13. Wagner, J. A., Lerrner, R. A. & Barbas, C. F. III Efficient aldolase catalytic antibodies that use the enamine mechanism of natural enzymes. *Science* **270,** 1797–1800 (1995).
14. Smithrud, D. B. & Benkovic, S. J. The state of antibody catalysis. *Curr. Opin. Biotechnol.* **8,** 459–466 (1997).
15. Lippard, S. J. & Berg, J. M. *Principles of Bioinorganic Chemistry* (University Science Books, Mill Valley, CA, 1994).
16. Walsh, C. T. & Orme-Johnson, W. H. Nickel enzymes. *Biochemistry* **26,** 4901–4906 (1987).
17. Watt, R. K. & Ludden, P. W. Nickel binding proteins. *Cell Mol. Life Sci.* **56,** 604–625 (1999).
18. Wong, C.-H. & Whitesides, G. M. *Enzymes in Synthetic Organic Chemistry* (Pergamon, Oxford, 1994).
19. Cane, D. (ed.) Thematic issue on polyketide and nonribosomal peptide synthases. *Chem. Rev.* **97,** 2463–2705 (1997).
20. Konz, D. & Marahiel, M. How do peptide synthetases generate structural diversity? *Chem. Biol.* **6,** R34–R38 (1999).
21. Cane, D. E., Walsh, C. T. & Khosla, C. Harnessing the biosynthetic code: combinations, permutations, and mutations. *Science* **282,** 63–68 (1998).
22. Trauger, J., Kohli, R. M., Mootz, H., Marahiel, M. & Walsh, C. Peptide cyclization catalysed by the thioesterase domain of tyrocidine synthetase. *Nature* **407,** 215–218 (2000).
23. Roach, P. L. *et al.* The crystal structure of isopenicillin N synthase, first of a new structural family of enzymes. *Nature* **375,** 700–704 (1995).
24. Valegard, K. *et al.* Structure of a cephalosporin synthase. *Nature* **394,** 805–809 (1998).
25. Que, L. One motif—many different reactions. *Nature Struct. Biol.* **7,** 182–184 (2000).
26. SinhaRoy, R., Milne, J., Belshaw, P., Gehring, A. & Walsh, C. Oxazole and thiazole peptide biosynthesis. *Nat. Prod. Rep.* **16,** 249–263 (1999).
27. Lewis, R. *et al.* Molecular mechanisms of drug inhibition of DNA gyrase. *BioEssays* **18,** 661–671 (1996).
28. Quadri, L. E., Keating, T. A., Patel, H. M. & Walsh, C. Assembly of the *Pseudomonas aeruginosa* nonribosomal peptide siderophore pyochelin: in vitro reconstitution of aryl-2,4-bis-thiazoline synthetase activity from PchD, E and F. *Biochemistry* **38,** 14941–14954 (1999).
29. Gehring, A., Mori, I., Perry, R. & Walsh, C. The nonribosomal peptide synthetase HMWP2 forms a thiazoline ring during biogenesis of yersiniabactin, an iron-chelating virulence factor of *Yersinia pestis*. *Biochemistry* **37,** 11637–11650 (1998).
30. Babbit, P. C. *et al.* The enolase superfamily: a general strategy for enzyme-catalyzed abstraction of the alpha-protons of carboxylic acids. *Biochemistry* **35,** 16489–16501 (1996).
31. Gerlt, J. A. & Babbit, P. C. Mechanistically diverse enzyme superfamilies: the importance of chemistry in the evolution of catalysis. *Curr. Opin. Chem. Biol.* **2,** 607–612 (1998).
32. Hubbard, B. K. Functional and mechanistic investigations of enzymes in the enolase superfamily. Thesis, Univ. Illinois (2000)
33. Tobin, M. B., Gustafsson, C. & Huisman, G. W. Directed evolution: the rational basis for irrational design. *Curr. Opin. Struct. Biol.* **10,** 421–427 (2000).
34. Schmidt-Dannert, C., Umeno, D. & Arnold, F. Molecular breeding of carotenoid biosynthetic pathways. *Nature Biotechnol.* **18,** 750–753 (2000).
35. Madison, L. L. & Huisman, G. J. Metabolic engineering of poly(3-hydroxyalkanoates): from DNA to plastic. *Microbiol. Mol. Biol. Rev.* **63,** 21–53 (1999).
36. Wackett, L. P. *et al.* Predicting microbial degradation pathways. *Am. Soc. Microbiol. News* **65,** 87–94 (1999).
37. McDaniel, R., Ebert-Khosla, S., Hopwood, D. A. & Khosla, C. Rational design of aromatic polyketide products by recombinant assembly of enzymatic subunits. *Nature* **375,** 549–554 (1995).
38. Bizily, S. P., Rugh, C. L., Summers, A. O. & Meagher, R. B. Phytoremediation of methylmercury pollution: *merB* expression in *Arabidopsis thaliana* confers resistance to organomercurials. *Proc. Natl Acad. Sci. USA* **96,** 6808–6813 (1999).

Acknowledgements

Work cited from the author's laboratory has been supported by the National Institutes of Health. I thank B. Hubbard for drawing the artwork in figures 1–7.